# GERMLINE-GOVERNED RECOGNITION OF A CANCER EPITOPE BY AN IMMUNODOMINANT HUMAN T-CELL RECEPTOR

David K Cole[1,2], Fang Yuan[1,3], Pierre J Rizkallah[1,2,4], John J Miles[2,5], Emma Gostick[2], David A Price[2], George F Gao[6], Bent K Jakobsen[7] and Andrew K Sewell[2]

[1]These authors contributed equally to this work.

[2]Department of Medical Biochemistry & Immunology, Henry Wellcome Building, Cardiff University School of Medicine, Heath Park, Cardiff, CF14 4XN, UK; [3]Nuffield Department of Clinical Medicine, John Radcliffe Hospital, Oxford University, Oxford, OX3 9DU, UK; [4]CLIK, STFC Daresbury Laboratory, Warrington, Cheshire, WA4 4AD, UK; [5]Cellular Immunology Laboratory, Queensland Institute of Medical Research, University of Queensland, Brisbane 4029, Australia; [6]Institute of Microbiology, Chinese Academy of Sciences, Beijing, PR China; [7]Immunocore Limited, 57C Milton Park, Abingdon, Oxon, OX14 4RX, UK.

Running head: Innate-like recognition by a human T-cell receptor

Address correspondence to: Professor Andrew Sewell. E-mail: sewellak@cardiff.ac.uk. Phone: +44(0)29 206 87055. Fax: +44(0)29 206 87007.

**CD8^{+} T-cells specific for MART-1$_{26-35}$, a dominant melanoma epitope restricted by human leukocyte antigen (HLA)-A\*0201, are exceptionally common in the naïve T-cell repertoire. Remarkably, the *TRAV12-2* gene is used to encode the T-cell receptor (TCR) $\alpha$ chain in >87% of these T-cells. Here, the molecular basis for this genetic bias is revealed from the structural and thermodynamic properties of an archetypal *TRAV12-2* encoded TCR complexed to the clinically relevant heteroclitic peptide, ELAGIGILTV, bound to HLA-A\*0201 (A2-ELA). Unusually, the *TRAV12-2* germline encoded regions of the TCR dominate the major atomic contacts with the peptide at the TCR/A2-ELA interface. This 'innate' pattern of antigen recognition likely explains the unique characteristics and extraordinary frequencies of CD8^{+} T-cell responses to this epitope.**

Malignant melanoma is responsible for 75% of all skin cancer-related deaths worldwide and the global incidence is rising. The MART-1 (1) protein, also known as Melan-A (2), is expressed by virtually all fresh melanoma tumor specimens and elicits natural CD8^{+} T-cell responses (3,4) that can lead to spontaneous disease regression (reviewed in (5)). Consequently, CD8^{+} T-cell responses directed against the MART-1 protein have been investigated extensively (reviewed in (2,6,7)) and heteroclitic forms of the dominant MART-1$_{26-35}$ peptide epitope (8,9), which is restricted by human leukocyte antigen (HLA)-A\*0201, are currently being used in a number of

clinical trials (10-12). In recent developments, adoptive T-cell therapy directed against the MART-1 protein has been used to mediate cancer regression in approximately 50% of late stage melanoma patients (13). However, these approaches have not proved to be universally effective and there remains considerable scope for improvement. In order to design more effective immune-based therapies against the MART-1 protein, it is essential to understand the precise molecular rules that govern the interaction between T-cell receptors (TCRs) and the HLA-A\*0201/MART-1$_{26-35}$ complex. Previous structural studies of human TCR/peptide-major histocompatibility complex (pMHC) interactions (14-16) indicate that specific regions of the TCR have different roles during antigen engagement; thus, the germline encoded complementarity determining region (CDR)1 and CDR2 loops contact mainly the conserved helical region of the MHC surface and the more variable somatically rearranged CDR3 loops contact mainly the antigenic peptide. Dissecting the nature of these contacts, which have been shown to be highly variable for individual TCR/pMHC interactions (17-19), is an important step towards understanding the principles of antigen recognition and for the development of improved T-cell vaccines (20). However, the current database of human TCR/pMHC complexes reported in the literature is limited (~16), compared with >100 antibody-antigen structures. This has made it difficult to ascertain whether there are conserved binding modes for TCR/pMHC interactions dictated by a number of specific contacts or

whether there are potentially unlimited numbers of TCR docking orientations dependent on the nature of individual recognition events. Furthermore, there are no examples to date of human TCR/pMHC class I structures in which the bound peptide is a decamer; this represents a substantial deficiency in our current knowledge given the preponderance with which decamer peptides are processed, presented and recognized. The low number of TCR/pMHC complex structures solved to date reflects technical difficulties inherent in the production of soluble TCR and pMHC molecules that retain stability and challenges related to the crystallization of complexes with relatively low binding affinities ($K_D = 0.1 - 112$ μM) (21,22). In general, TCRs specific for tumor-derived epitopes bind in the weaker range of TCR/pMHC affinities (21). This obstacle to the generation of high quality co-complex crystals is underscored by the fact that only one other tumor-specific human TCR/pMHCI complex structure has been documented previously (23).

In this study, we expressed a soluble TCR (MEL5) specific for ELAGIGILTV, the common MART-$1_{26-35}$ heteroclitic peptide, complexed to HLA-A*0201 (A2-ELA). Notably, HLA-A*0201 is the most common HLA allele in the human population (24). The CDR1 and CDR2 loops of this TCR are encoded by the *TRAV12-2* and *TRBV30* genes (IMGT nomenclature). Interestingly, the *TRAV12-2* gene is expressed in the vast majority of CD8^{+} T-cell populations specific for HLA-A*0201/MART-$1_{26-35}$ across multiple individuals (25,26). To resolve the enigma of the dominant *TRAV12-2* gene and determine the molecular characteristics that govern CD8^{+} T-cell recognition of the HLA-A*0201/MART-$1_{26-35}$ antigen, we performed a biophysical, thermodynamic and structural analysis of MEL5 TCR binding to A2-ELA. The data provide a molecular basis for biased TCR gene product selection in the CD8^{+} T-cell response to HLA-A*0201/MART-$1_{26-35}$ and indicate that pMHC antigens can be subject to "innate-like" binding modes within adaptive immune responses.

**Experimental Procedures**

*Generation of CD8^{+} T-cell clones specific for HLA-A*0201/MART-1$_{26-35}$*

CD8^{+} T-cell clones were generated as described previously (27). Briefly, peripheral blood mononuclear cells, isolated from an HLA-A*0201^{+} healthy donor, were stimulated with 1 nM ELAGIGILTV peptide and cloned via limiting dilution. These cells were then screened for A2-ELA tetramer binding. The MEL5 CD8^{+} T-cell clone isolated from these experiments activated typically in response to HLA-A*0201^{+} target cells pulsed with the ELAGIGILTV peptide, exhibiting specific degranulation (CD107a mobilization) and the production of interferon-γ, interleukin-2 and tumor necrosis factor-α (data not shown). The MEL5 TCR was derived from the MEL5 CD8^{+} T-cell clone. Two independent CD8^{+} T-cell clones grown in the same way, MEL11 and MEL13, were shown to express an identical TCR.

*Generation of expression plasmids*
The MEL5 TCR, HLA-A*0201 α chain and β2m sequences were generated by PCR mutagenesis (Stratagene) and PCR cloning. All sequences were confirmed by automated DNA sequencing (Lark Technologies). For MEL5, a disulphide linked construct was used to produce the soluble domains (variable and constant) for both the α and β chains (28,29). The soluble HLA-A*0201 α chain (α1, α2 and α3 chain domains), tagged with a biotinylation sequence, and β2m were also cloned and used to make the HLA-A*0201 protein. The TCR, HLA-A*0201 α chain and β2m sequences were inserted into separate pGMT7 expression plasmids under the control of the T7 promoter (28).

*Protein expression, refolding and purification*
Competent Rosetta DE3 *E.coli* cells were used to produce the MEL5 α and β chains, and the HLA-A*0201 α and β2m chains, in the form of inclusion bodies (IBs) using 0.5 mM IPTG to induce expression as described previously (28). For a 1 L refold, 30 mg of MEL5 α chain IBs were incubated at 37°C for 15 mins with 10 mM DTT and added to cold refold buffer (50 mM TRIS pH 8.1, 2 mM EDTA, 2.5 M urea, 6 mM cysteamine hydrochloride and 4 mM cystamine). After 15 mins, 30 mg of MEL5 β chain, incubated at 37°C for 15 mins with 10 mM DTT, was added. For a 1 L A2-ELA refold, 30 mg of α chain was mixed with 30 mg of β2m and 4 mg of the

ELAGIGILTV peptide at 37°C for 15 mins. This was then added to cold refold buffer (50 mM TRIS pH 8, 2 mM EDTA, 400 mM L-arginine, 6 mM cysteamine hydrochloride and 4 mM cystamine). Refolds were mixed at 4°C for >1 h. Dialysis was carried out against 10 mM TRIS pH 8.1 until the conductivity of the refolds was under 2 mS/cm. The refolds were then filtered in preparation for the purification steps. Refolded proteins were purified initially by ion exchange using a Poros50HQ™ column and finally gel filtered into BIAcore buffer (10 mM HEPES pH 7.4, 150 mM NaCl, 3 mM EDTA and 0.005% (v/v) Surfactant P20) or crystallization buffer (10 mM TRIS pH 8.1, 10mM NaCl) using a Superdex200HR™ column. Protein quality was analyzed by Coomassie-stained SDS-PAGE.

### pMHC biotinylation
Biotinylated pMHC was prepared as described previously (30).

### Surface plasmon resonance (SPR) analysis
Binding analysis was performed independently using a BIAcore T100™ equipped with a CM5 sensor chip as reported previously (31). Between 200 and 400 response units (RUs) of biotinylated pMHC was immobilized to streptavidin, which was chemically linked to the chip surface. The pMHC was injected at a slow flow rate (10 μl/min) to ensure uniform distribution on the chip surface. Combined with the small amount of pMHC bound to the chip surface, this reduced the likelihood of off-rate limiting mass transfer effects. MEL5 was purified and concentrated to ~100 μM on the same day of SPR analysis to reduce the likelihood of TCR aggregation affecting the results. For equilibrium and kinetic analysis, ten serial dilutions were carefully prepared in triplicate for each sample and injected over the relevant sensor chips at 25°C. MEL5 was injected over the chip surface using kinetic injections at a flow rate of 45 μl/min. For the thermodynamic experiments, this method was repeated at the following temperatures; 5ºC, 13ºC, 21ºC, 25ºC, 29ºC and 37ºC. Results were analyzed using BIAevaluation 3.1™, Microsoft Excel™ and Origin 6.1™. The equilibrium binding constant ($K_D$) values were calculated using a nonlinear curve fit ($y = (P_1x)/(P_2 + x)$). The thermodynamic parameters were calculated using the Gibbs equation ($y=dH+dCp*(x-298)-x*dS-x*dCp*\ln(x/298)$).

### Crystallization
The MEL5/A2-ELA complex was crystallized as reported previously (32).

### Diffraction data collection and model refinement
A data set up to 3.0Å was collected with the rotation method at SRS Station 14.2, Daresbury, UK using an ADSC Quantum 4 CCD-detector system. The wavelength (λ) was set to 0.979 Å. A total of 160 frames were recorded, each covering 0.5° of rotation. The crystal was maintained at 100ºK in an Oxford Cryostream. Reflection intensities were estimated with the MOSFLM package (33) and the data were scaled, reduced and analyzed with SCALA and the CCP4 package (34). The structure was solved with molecular replacement using PHASER (35). Despite close similarity to NY-ESO-1 complexes solved recently, e.g. 2P5E or 2P5W, a solution could be obtained only with a composite search model constructed with CHAINSAW as follows: the HLA-A*0201 α chain (A) was taken from 2F53, the β2m chain (B) was taken from 2BCK, the TCR α chain (D) was taken from 1AO7 and the TCR β chain (E) was taken from 2F53. The peptide was not included at this stage, as it was only a small fraction of the diffracting material. The model sequence was adjusted with COOT (36) and the model refined with REFMAC5, version 5.2.0019 (37). The model was split into eight domains for TLS refinement (A2α1α2, A2α3, β2m, ELA peptide, MEL5α constant, MEL5α variable, MEL5β constant and MEL5β variable). After convergence, one round of restrained thermal parameters was completed, in order to obtain the full B-values for atoms. Graphical representations were prepared with PYMOL (38). Data collection and reduction statistics, and refinement statistics, are shown in Table 1. The final model coordinates were deposited with the PDB database, assigned accession code 3HG1.

## Results

### Structure determination and analysis of MEL5 in complex with A2-ELA

To investigate the structural basis for dominant *TRAV12-2* gene usage in CD8^{+} T-cell populations specific for HLA-A*0201/MART-1$_{26-35}$, we solved the atomic structure of MEL5 in complex with A2-ELA (Table 1; Figure 1A). Molecular replacement was successful only in space group P4$_3$, consistent with the presence of one molecule of the complex per asymmetric unit, and the resolution was sufficiently high to show that the interface between the two molecules was well ordered and contained well defined electron density. The final model showed ~96% of residues in the preferred and allowed regions of the Ramachandran plot and geometry consistent with the data resolution. The crystallographic R/Rfree factors were 22.5% and 30.4%. There was enough ordered density around the protein model to allow the identification of 2 glycerol molecules, 2 sulphate ions and 44 solvent (water) molecules. The C-terminus of the TCR α chain was disordered beyond residue 195, with no apparent electron density beyond that point.

The MEL5 docking angle with A2-ELA was 35° (calculated as in (14)), with the TCR α chain contacting the α2 domain and the TCR β chain contacting the α1 domain of A2-ELA (Figure 1A – C ). The docking angle in this complex lies within the range observed for other human TCR/pMHC complexes, with the A6 TCR/A2-Tax complex representing one extreme (32°) (28) and the 1G4 TCR/A2-NY-ESO (23) complex representing the other extreme (69°). The TCR was located towards the N-terminus of the MHC peptide binding groove, as observed in the A6 TCR/A2-Tax and B7 TCR/A2-Tax complexes (39,40), and centred over the solvent exposed bulge of the ELA peptide (Figure 1B – C).

The total buried surface area of the interaction was approximately 1226 Å$^2$, the lowest for any human TCR/pMHC interaction reported to date. This supports the observation that MEL5 makes significantly fewer contacts with the pMHC surface compared to other TCR/pMHCI complexes, which indicates that T-cell recognition of antigen can occur with a lower number of specific contacts than previously thought. Although the ELA peptide is a decamer, the contribution of the peptide (29% of the interface area) to TCR binding was within the normal range observed for other TCR/pMHCI complexes (18-34%) that typically contain nonamers in the peptide binding groove. The contribution of the TCR α and TCR β chains has been shown to vary markedly for different human TCR/pMHC complexes, the largest difference being observed for the JM22 TCR/A2-Flu complex (41) (α chain – 33%, β chain – 67%). For the MEL5/A2-ELA complex, the interaction was split relatively evenly (α chain – 50.4%, β chain – 49.6%). The surface complementarity (SC) across the interface as a whole was 0.63, with a slightly lower score of 0.58 between the MHC and the TCR alone. However, the score increased to 0.76 when the TCR and the peptide interface were considered, indicating a much closer and more directed match.

### *MEL5/A2 contacts*

MEL5 forms 12 contacts, comprising 9 electrostatic interactions and 3 van der Waals (vdW) close interactions, with the conserved MHC α helices of HLA-A*0201 that constitute the sides of the peptide binding groove (Table 2). These contacts are dominated by the CDR1α loop, which is located over the N-terminus of the ELA peptide and makes a significant contribution to the TCR/MHC α2 helix interface, forming a dense network of 4 electrostatic interactions between the TCR α chain residue Arg28 and the MHC α2 residues Glu166 and Trp167. Notably, the CDR1β loop plays no part in contacting the A2-ELA antigen (Table 2). Further contacts were evident between the MHC α1 helix and the TCR CDR3α, CDR2β and CDR3β loops as detailed in Table 2. A number of conserved, or 'gatekeeper' interactions, that are present in the majority of TCR/pMHCI complex structures solved to date (14), were also present between MEL5 and the MHC surface. These include electrostatic interactions between the TCR residue Glu59 and the MHC residue Arg65, and between the TCR residues Gly99 and Thr100 and the MHC residue Gln155. Interestingly, MEL5 does not contact MHC α1 domain residue Arg69, or Gln72 that represents the other 'gatekeeper' TCR/MHC contact (14).

### *A2-ELA conformation in uncomplexed and TCR-complexed forms*

The crystal structure of uncomplexed A2-ELA has been solved (42). Although the ELA peptide is a decamer, it adopts a similar conformation to nonamer peptides with a central bulge between residues 4 to 6 (Figure 2A). In the case of the ELA peptide, the extra residue is accommodated, not through a more prominent central bulge, but by an extension of the peptide Cα chain towards the α2 domain of the HLA-A*0201 binding groove. Superposition of the uncomplexed A2-ELA and the MEL5-complexed A2-ELA structures shows that the peptide termini are located at virtually identical positions. This peptide conformation results in the availability of a number of residues for specific TCR contacts; these include GluP1, LeuP2, AlaP3, GlyP4, IleP5, GlyP6, IleP7, LeuP8 and ThrP9 (Figure 2). Compared with the uncomplexed A2-ELA structure, the conformation of the ELA peptide upon docking with the TCR is very similar, with a root mean squared deviation (RMSD) value of 0.369 between the peptides in uncomplexed and TCR-complexed forms. There are some conformation differences in the side chains of LeuP8, and ThrP9, which adopt visually different conformations in the uncomplexed A2-ELA structure; however, these differences are within experimental error, and may not represent changes in peptide conformation due to stabilization of the peptide upon TCR docking.

### The dominant role of the TRAV12-2 encoded CDR1 loop during peptide binding

MEL5 contacts 8 of the A2-ELA peptide residues (Table 2, Figure 2B), compared with only 3 for the immunodominant LC13 TCR/B8-EBNA (43) and the JM22 TCR/A2-Flu (41) complexes. Unusually, the CDR3α loop has a minimal role in contacting the ELA peptide, making only one electrostatic interaction between TCR residue Asn92 and the ELA peptide at GlyP4. A substantial number of contacts at the interface are formed between Gln31 in the CDR1α loop, encoded by the *TRAV12-2* gene, and the antigenic peptide (Table 2). The Gln31 residue makes a dense network of contacts to GluP1, LeuP2, GlyP4 and IleP5 and is therefore likely to have a chief role in peptide recognition (Table 2; Figure 2B). In this unusual TCR binding mode, the CDR1α loop acts comparably to that of a classical CDR3 loop with respect to peptide contacts. The dominance of the CDR1α loop in

terms of contacting both the surface of HLA-A*0201 and the bound ELA peptide could explain the prevalent expression of the *TRAV12-2* gene in CD8^{+} T-cell responses specific for MART-1$_{26-35}$ (26). Furthermore, the *TRAV12-2* gene, which encodes the CDR1α and CDR2α loops of MEL5, is also expressed by the A6 TCR, which is specific for the Tax$_{11-19}$ peptide (LLFGYPVYV) bound to HLA-A*0201 (A2-Tax) (28). The CDR1α and CDR2α loops of the A6 TCR utilize a virtually identical antigen binding mode to that seen in the MEL5/A2-ELA complex, with both TCRs making contacts between CDR1α loop residue Arg28 and MHC α2 residue Trp167, and CDR1α loop residue Gln31 and peptide positions 1 and 4 (GluP1 and GlyP4 for A2-ELA; LeuP1 and GlyP4 for A2-Tax) (Figure 3). In all other published TCR/pMHC complexes, the CDR1α and CDR2α loops, which are not encoded by the *TRAV12-2* gene, form unique contacts with their respective pMHC complexes compared with the MEL5/A2-ELA complex; this observation lends credence to the idea that TCRs expressing the *TRAV12-2* gene could have a selective advantage when binding to cognate antigen restricted by HLA-A*0201 due to germline encoded, or "innate" recognition, of residues on the MHC surface and in the bound peptide. Consequently, although the TCRα and TCRβ chains contribute relatively equally in both the A6 TCR and MEL5 complexes, the conservation in the position of the TCRα chain in both complexes indicates that the A6 TCR and MEL5 bind to their cognate pMHCs in an "α-centric" manner; i.e. the binding position of these TCRs is governed by the α chain.

### The role of the TCRβ chain during peptide binding

The TCRβ chain utilizes a classical peptide binding mode, interacting with the ELA peptide solely through contacts made by the CDR3β loop. In total, the CDR3β loop makes 5 hydrogen bonds and 5 vdW interactions between Thr96, Leu98 and Gly99 of the TCR and AlaP3, GlyP4, IleP5, GlyP6, IleP7 and ThrP9 of the peptide. However, all of the hydrogen bonds, which constitute the majority of the binding energy, are located between the CDR3β loop and the C-terminus of the peptide (GlyP6, IleP7 and ThrP9).

Interestingly, the position of the CDR3β loop enables a dense network of interactions, including 3 hydrogen bonds, between TCR residues Leu98 and Gly99 and peptide residue IleP7. These contacts are noteworthy because the side chain of IleP7 acts like an anchor, pointing down towards the MHC surface, thereby making it an unusual candidate for TCR binding. Thus, the contacts between the CDR3β loop and the ELA peptide contribute significantly to the binding stability of the MEL5/A2-ELA complex.

### Binding affinity and thermodynamics of the MEL5/A2-ELA complex

We have previously shown that MEL5 binds to A2-ELA with a comparatively weak affinity and extremely fast kinetics compared with other TCR/pMHC interactions ($K_D = 18\mu M$; kinetics too fast to measure) (21). To investigate the thermodynamic properties of this interaction, we measured the binding of MEL5 to A2-ELA at 5ºC, 13ºC, 21ºC, 25ºC, 29ºC and 37ºC using a BIAcore T100™ (Figure 4, Table 3). The affinity of the MEL5/A2-ELA interaction increased from $K_D = 26.9\ \mu M$ at 5ºC to $K_D = 17.3\ \mu M$ at 37ºC (Figure 4A – F). The affinity data was plotted as binding $\Delta G_0$ versus temperature using nonlinear regression to fit the three-parameter equation to the curve in order to calculate $\Delta H_0$, $T\Delta S_0$ and $\Delta Cp_0$ (Figure 4G). At 25ºC, the MEL5/A2-ELA interaction was characterized by a $\Delta G_0$ of -6.5 kcal/mol, which is within the normal range for TCR/pMHC interactions (Table 3). The MEL5/A2-ELA interaction is strongly entropically driven, with a favorable $T\Delta S_0$ of 8.3 kcal/mol. This favorable entropy is likely to be derived mainly from the expulsion of ordered water molecules upon complex formation, allowing the TCR to contact the pMHC surface directly and form the electrostatic and vdW interactions evident in the co-complex structure. Interestingly, this is the first published instance of a TCR/pMHC interaction that is enthalpically unfavorable, with a $\Delta H_0$ of 2 kcal/mol. This indicates that there is a net decrease in the number of favorable non-covalent bonds (hydrogen bonds, vdW contacts) during complex formation and reinforces the importance of the favourable entropic contribution to the binding of MEL5 to A2-ELA. Furthermore, this observation could explain the extremely fast kinetics of the MEL5/A2-ELA interaction; i.e. the net loss of bond formation could lead to the observed low stability, and hence the fast off-rate, of the complex. During complex formation, there is normally a net increase in the total buried surface area, which results in a negative $\Delta Cp_0$ value. In the case of the MEL5/A2-ELA interaction, however, a relatively small $\Delta Cp_0$ value (-0.14 kcal/mol·K) was observed compared with other TCR/pMHC complexes. This supports the observation that the total buried surface area of 1226 Å$^2$ for the MEL5/A2-ELA complex is the smallest reported to date for any TCR/pMHC complex.

### Discussion

Here, we report the structure of an archetypal *TRAV12-2* encoded TCR (MEL5), derived from a CD8$^+$ T-cell clone specific for MART-1$_{26-35}$, in complex with A2-ELA; A2-ELA is currently the most studied heteroclitic peptide in the literature, and is central to a number of clinical trials (10-12). Although the A2-ELA peptide (E**L**AGIGILTV) is a heteroclitic version of the MART-1$_{26-35}$ peptide (E**A**AGIGILTV), structural evidence suggests that the substitution of Ala to Leu at the peptide anchor position 2 does not substantially alter the peptide conformation (42,44). Thus, an understanding of the molecular basis for T-cell recognition of this antigen should inform the rational improvement of current melanoma therapies.

Previous investigations have shown that CD8$^+$ T-cells engage the HLA-A*0201/MART-1$_{26-35}$ antigen with predictable TCR gene usage patterns (26,45). Thus, these particular TCRs show classic class II bias (shared *TRBV* and/or *TRAV* usage among individuals bearing the same MHCI allele) and class III bias (identical TCRs among individuals bearing the same MHCI allele) (46); interestingly, they can also be detected both in tumor-infiltrated lymph nodes (TILNs) and in the blood of healthy individuals and newborns (26,45). The most striking example of TCR gene bias occurs for the *TRAV* gene segment; thus, in which, of the 53 CD8$^+$ T-cell clones that have been raised against the HLA-A*0201/MART-1$_{26-35}$ antigen, 47 (87%) use the *TRAV12-2* gene (26). Since the *TRAV12-2* gene is only expressed on the surface of ~3% of circulating lymphocytes (47), the very high prevalence of *TRAV12-2* usage in

6

these melanoma-specific CD8$^+$ T-cell responses indicates that this particular gene is advantageous during antigen-driven selection. The *TRAV12-2* encoded regions of the MEL5 TCR play a dominant role at both the peptide and MHC interface. The CDR1$\alpha$ residue Arg28 helps to fix the TCR to the MHC $\alpha$2 helix via 4 electrostatic interactions, while the CDR1$\alpha$ residue Gln31 appears integral to peptide recognition through 2 vdW bonds and 4 electrostatic interactions to GluP1, LeuP2, GlyP4 and IleP5. In general, the CDR1$\alpha$ loop plays a role comparable to the CDR3 loop in other TCR/pMHC structures given its central position above the N-terminus of the peptide and the extensive binding networks between the CDR1$\alpha$ loop and bound peptide. It is striking to note that residues encoded by the *TRAV12-2* gene make 9/19 of the electrostatic interactions with A2-ELA, more than any of the other TCR regions in this structure. Furthermore, when the bonding networks are taken into account, it becomes clear why the *TRAV12-2* subfamily is heavily selected *in vivo.* For instance, only 3/47 *TRAV* genes encode Arg at position 28 and only 3/47 *TRAV* genes encode Gln at position 31; only the *TRAV12-2* gene encodes both. In fact, even the highly homologous sister genes of *TRAV12-2*, specifically *TRAV12-1* and *TRAV12-3*, could not likely be substituted given that they encode a polar, uncharged Ser at position 28. This single substitution would likely result in the loss of 4 electrostatic interactions at the pMHC interface. In support of this idea, no TCRs specific for the HLA-A*0201/MART-1$_{26-35}$ complex have so far been found that use either the *TRAV12-1* or the *TRAV12-3* genes (26). Thus, the dominant selection of this "quasi-innate", self-reactive TCR likely represents an advantageous role during host responses against the HLA-A*0201/MART-1$_{26-35}$ antigen that cannot be fulfilled by TCRs of alternate specificities.

Further inspection of the MEL5/A2-ELA complex reveals additional features that could contribute to the dominant expression of the *TRAV12-2* encoded CDR1$\alpha$ loop in CD8$^+$ T cell responses specific for HLA-A*0201/MART-1$_{26-35}$. Strikingly, MEL5 contacts primarily the main chain of the ELA peptide; indeed, only 3/17 peptide contacts are side chain interactions. This is disparate from the

more equal distribution of side chain versus main chain peptide interactions observed in most other TCR/pMHC structures and implies that MEL5 may be less sensitive to peptide sequence relative to peptide conformation. Moreover, the somatically rearranged CDR3$\beta$ loop principally utilizes main chain atoms to contact the peptide, whereas the germline encoded CDR1$\alpha$ loop uses predominantly side chain atoms to contact the peptide. This interesting dichotomy of binding strategies between the CDR3$\beta$ and CDR1$\alpha$ loops in the MEL5/A2-ELA complex may have implications for antigen specificity; thus, changes in the sequence of the CDR3$\beta$ loop may be tolerated when binding to A2-ELA as long as the overall conformation of the loop is maintained, whereas changes in the sequence of the CDR1$\alpha$ loop may disrupt T-cell recognition of A2-ELA due to loss of side-chain specific interactions.

Interestingly, the *TRAV12-2* gene is also used by the A6 TCR, which is specific for the A2-Tax complex; this is the first structural example in which an identical gene is shared between TCRs specific for a tumor antigen (MEL5/A2-ELA) and a viral antigen (A6 TCR/A2-Tax). In both of these TCR/pMHCI complexes, the *TRAV12-2* gene encoded CDR1$\alpha$ loops are suspended over the N-terminus of their respective cognate pMHCI molecules. This feature enables the CDR1$\alpha$ loops of each TCR to form far more contacts with the antigenic peptide compared to the corresponding CDR3$\alpha$ loops. In both complexes, the CDR$\beta$ domains conform to the classical model of TCR/pMHC binding, with the CDR2$\beta$ loop contributing mainly to MHC contacts and the CDR3$\beta$ loop contributing mainly to peptide interactions. Furthermore, despite the fact that MEL5 and the A6 TCR are encoded by unique TCR$\beta$ chain genes (*TRBV30* and *TRBV6-5* respectively), the TCRs align in virtually identical positions and orientations over the respective cognate pMHCI molecules in both the MEL5/A2-ELA and the A6 TCR/A2-Tax complexes, thereby indicating that the TCR$\alpha$ chain encoded by the *TRAV12-2* gene has a dominant role during TCR/pMHCI docking compared with the TCR$\beta$ chain. This observation lends support to the idea that MEL5 and the A6 TCR are "$\alpha$-centric"; i.e. their binding orientation is governed by common

contacts between the TCRα chain and the MHC surface (18). Moreover, despite the unique sequences of the peptides in the A2-ELA (ELAGIGILTV) and A2-Tax (LLFGYPVYV) complexes, the binding mode implemented by the CDR1α loop encoded by the germline *TRAV12-2* gene in both the MEL5/A2-ELA complex and the A6 TCR/A2-Tax complex is virtually identical; thus, contacts between the CDR1α loop residue Arg28 and the MHC α2 residue Trp167 and, most notably, between the CDR1α loop residue Gln31 and peptide positions 1 and 4 (GluP1 and GlyP4 for A2-ELA; LeuP1 and GlyP4 for A2-Tax) are evident in both complex structures (Figure 3C – D). Thus, the specificity of MEL5 for the HLA-A*0201/MART-1[26-35] antigen is achieved not only through the highly variable somatically rearranged CDR3 loops, as observed for other TCR/pMHC complexes, but also through the germline derived CDR1α loop, which contributes significantly to peptide binding. Although considerable contacts between the TCR CDR1 loops and the antigenic peptide have been observed in some other TCR/pMHC complexes (48), this is the first example of specific antigen recognition via identical germline-encoded receptor loops shared by both anti-viral (A6 TCR/A2-Tax) and anti-self (MEL5/A2-ELA) T-cells.

In summary, this first structure of a human TCR in complex with a decamer peptide bound to MHCI considerably extends our knowledge of TCR/pMHC interactions. First, the MEL5/A2-ELA interaction is the only enthalpically unfavourable TCR interaction ever described (49). Second, the MEL5/A2-ELA complex has the lowest buried surface area (1226 $\text{Å}^2$) of any published TCR/pMHC complex, an observation that is supported by the relatively small $\Delta Cp_0$ value (-0.14 kcal/mol K). Third, this structure shows that the specificity of MEL5 for A2-ELA is achieved in large part through interactions with the CDR1α loop, which contributes significantly to peptide binding and is akin to that of classical CDR3 loops during pMHC binding. The dominance of the germline-encoded regions in this α-centric TCR during pMHC binding indicates an important role for the *TRAV12-2* gene product in antigen recognition. Thus, TCRs that use the *TRAV12-2* gene may enable CD8^{+} T-cells to recognize and respond to the HLA-A*0201/MART-1[26-35] antigen through a "quasi-innate" recognition system. These observations likely explain the biased TCR usage that has been observed in CD8^{+} T-cell populations specific for HLA-A*0201/MART-1[26-35] and further reported in a variety of other human diseases (reviewed in (46,50)).

# References

1. Kawakami, Y., Eliyahu, S., Sakaguchi, K., Robbins, P. F., Rivoltini, L., Yannelli, J. R., Appella, E., and Rosenberg, S. A. (1994) *J Exp Med* **180**, 347-352

2. Romero, P., Valmori, D., Pittet, M. J., Zippelius, A., Rimoldi, D., Levy, F., Dutoit, V., Ayyoub, M., Rubio-Godoy, V., Michielin, O., Guillaume, P., Batard, P., Luescher, I. F., Lejeune, F., Lienard, D., Rufer, N., Dietrich, P. Y., Speiser, D. E., and Cerottini, J. C. (2002) *Immunol Rev* **188**, 81-96

3. Voelter, V., Rufer, N., Reynard, S., Greub, G., Brookes, R., Guillaume, P., Grosjean, F., Fagerberg, T., Michelin, O., Rowland-Jones, S., Pinilla, C., Leyvraz, S., Romero, P., and Appay, V. (2008) *Int Immunol* **20**, 1087-1096

4. Pittet, M. J., Valmori, D., Dunbar, P. R., Speiser, D. E., Lienard, D., Lejeune, F., Fleischhauer, K., Cerundolo, V., Cerottini, J. C., and Romero, P. (1999) *J Exp Med* **190**, 705-715

5. Chodorowski, Z., Anand, J. S., Wisniewski, M., Madalinski, M., Wierzba, K., and Wisniewski, J. (2007) *Przegl Lek* **64**, 380-382

6. Pittet, M. J., Zippelius, A., Valmori, D., Speiser, D. E., Cerottini, J. C., and Romero, P. (2002) *Trends Immunol* **23**, 325-328

7. Kawakami, Y., and Rosenberg, S. A. (1997) *Int Rev Immunol* **14**, 173-192

8. Speiser, D. E., Lienard, D., Pittet, M. J., Batard, P., Rimoldi, D., Guillaume, P., Cerottini, J. C., and Romero, P. (2002) *Eur J Immunol* **32**, 731-741

9. Valmori, D., Fonteneau, J. F., Lizana, C. M., Gervois, N., Lienard, D., Rimoldi, D., Jongeneel, V., Jotereau, F., Cerottini, J. C., and Romero, P. (1998) *J Immunol* **160**, 1750-1758

10. Bins, A., Mallo, H., Sein, J., van den Bogaard, C., Nooijen, W., Vyth-Dreese, F., Nuijen, B., de Gast, G. C., and Haanen, J. B. (2007) *J Immunother* **30**, 234-239

11. Chen, Q., Jackson, H., Shackleton, M., Parente, P., Hopkins, W., Sturrock, S., MacGregor, D., Maraskovsky, E., Tai, T. Y., Dimopoulos, N., Masterman, K. A., Luke, T., Davis, I. D., Chen, W., and Cebon, J. (2005) *Cancer Immun* **5**, 5

12. Meidenbauer, N., Marienhagen, J., Laumer, M., Vogl, S., Heymann, J., Andreesen, R., and Mackensen, A. (2003) *J Immunol* **170**, 2161-2169

13. Morgan, R. A., Dudley, M. E., Wunderlich, J. R., Hughes, M. S., Yang, J. C., Sherry, R. M., Royal, R. E., Topalian, S. L., Kammula, U. S., Restifo, N. P., Zheng, Z., Nahvi, A., de Vries, C. R., Rogers-Freezer, L. J., Mavroukakis, S. A., and Rosenberg, S. A. (2006) *Science* **314**, 126-129

14. Rudolph, M. G., Stanfield, R. L., and Wilson, I. A. (2006) *Annu Rev Immunol* **24**, 419-466

15. Tynan, F. E., Reid, H. H., Kjer-Nielsen, L., Miles, J. J., Wilce, M. C., Kostenko, L., Borg, N. A., Williamson, N. A., Beddoe, T., Purcell, A. W., Burrows, S. R., McCluskey, J., and Rossjohn, J. (2007) *Nat Immunol* **8**, 268-276

16. Armstrong, K. M., Piepenbrink, K. H., and Baker, B. M. (2008) *Biochem J* **415**, 183-196

17. Borg, N. A., Ely, L. K., Beddoe, T., Macdonald, W. A., Reid, H. H., Clements, C. S., Purcell, A. W., Kjer-Nielsen, L., Miles, J. J., Burrows, S. R., McCluskey, J., and Rossjohn, J. (2005) *Nat Immunol* **6**, 171-180

18. Feng, D., Bond, C. J., Ely, L. K., Maynard, J., and Garcia, K. C. (2007) *Nat Immunol* **8**, 975-983

19. Tynan, F. E., Borg, N. A., Miles, J. J., Beddoe, T., El-Hassen, D., Silins, S. L., van Zuylen, W. J., Purcell, A. W., Kjer-Nielsen, L., McCluskey, J., Burrows, S. R., and Rossjohn, J. (2005) *J Biol Chem* **280**, 23900-23909

20. Borbulevych, O. Y., Baxter, T. K., Yu, Z., Restifo, N. P., and Baker, B. M. (2005) *J Immunol* **174**, 4812-4820

21. Cole, D. K., Pumphrey, N. J., Boulter, J. M., Sami, M., Bell, J. I., Gostick, E., Price, D. A., Gao, G. F., Sewell, A. K., and Jakobsen, B. K. (2007) *J Immunol* **178**, 5727-5734

22. Varela-Rohena, A., Molloy PE, Dunn SM, Li Y, Suhoski MM, Carroll RG, Milicic A, Mahon T, Sutton DH, Laugel BE, Moysey R, Cameron BJ, Vuidepot A, Purbhoo ME, Cole DK, Phillips RE, June CH, Jakobsen BK, Riley JL and Sewell AK. (2008) *Nature Medicine* **1**, 4

23. Chen, J. L., Stewart-Jones, G., Bossi, G., Lissin, N. M., Wooldridge, L., Choi, E. M., Held, G., Dunbar, P. R., Esnouf, R. M., Sami, M., Boulter, J. M., Rizkallah, P., Renner, C., Sewell, A., van der Merwe, P. A., Jakobsen, B. K., Griffiths, G., Jones, E. Y., and Cerundolo, V. (2005) *J Exp Med* **201**, 1243-1255

24. Krausa, P., Brywka, M., 3rd, Savage, D., Hui, K. M., Bunce, M., Ngai, J. L., Teo, D. L., Ong, Y. W., Barouch, D., Allsop, C. E., and et al. (1995) *Tissue Antigens* **45**, 223-231

25. Trautmann, L., Labarriere, N., Jotereau, F., Karanikas, V., Gervois, N., Connerotte, T., Coulie, P., and Bonneville, M. (2002) *Eur J Immunol* **32**, 3181-3190

26. Dietrich, P. Y., Le Gal, F. A., Dutoit, V., Pittet, M. J., Trautman, L., Zippelius, A., Cognet, I., Widmer, V., Walker, P. R., Michielin, O., Guillaume, P., Connerotte, T., Jotereau, F., Coulie, P. G., Romero, P., Cerottini, J. C., Bonneville, M., and Valmori, D. (2003) *J Immunol* **170**, 5103-5109

27. Laugel, B., van den Berg, H. A., Gostick, E., Cole, D. K., Wooldridge, L., Boulter, J., Milicic, A., Price, D. A., and Sewell, A. K. (2007) *J Biol Chem* **282**, 23799-23810

28. Garboczi, D. N., Ghosh, P., Utz, U., Fan, Q. R., Biddison, W. E., and Wiley, D. C. (1996) *Nature* **384**, 134-141

29. Boulter, J. M., Glick, M., Todorov, P. T., Baston, E., Sami, M., Rizkallah, P., and Jakobsen, B. K. (2003) *Protein Eng* **16**, 707-711

30. Wyer, J. R., Willcox, B. E., Gao, G. F., Gerth, U. C., Davis, S. J., Bell, J. I., van der Merwe, P. A., and Jakobsen, B. K. (1999) *Immunity* **10**, 219-225

31. Cole, D. K., Dunn, S. M., Sami, M., Boulter, J. M., Jakobsen, B. K., and Sewell, A. K. (2008) *Mol Immunol* **45**, 2700-2709

32. Yuan, F., Georgiou, T., Hillon, T., Gostick, E., Price, D. A., Sewell, A. K., Moysey, R., Gavarret, J., Vuidepot, A., Sami, M., Bell, J. I., Gao, G. F., Rizkallah, P. J., and Jakobsen, B. K. (2007) *Acta Crystallogr Sect F Struct Biol Cryst Commun* **63**, 758-760

33. Leslie, A. G. W. (1992) *Joint CCP4 + ESF-EAMCB Newsletter on Protein Crystallography* **26**

34. Collaborative Computational Project, N. (1994) *Acta Crystallogr D Biol Crystallogr* **50**, 760-763

35. McCoy, A. J., Grosse-Kunstleve, R. W., Storoni, L. C., and Read, R. J. (2005) *Acta Crystallogr D Biol Crystallogr* **61**, 458-464

36. Emsley, P., and Cowtan, K. (2004) *Acta Crystallogr D Biol Crystallogr* **60**, 2126-2132

37. Murshudov, G. N., Vagin, A. A., and Dodson, E. J. (1997) *Acta Crystallogr D Biol Crystallogr* **53**, 240-255

38. DeLano, W. L. (2002)

39. Ding, Y. H., Smith, K. J., Garboczi, D. N., Utz, U., Biddison, W. E., and Wiley, D. C. (1998) *Immunity* **8**, 403-411

40. Ding, Y. H., Baker, B. M., Garboczi, D. N., Biddison, W. E., and Wiley, D. C. (1999) *Immunity* **11**, 45-56

41. Stewart-Jones, G. B., McMichael, A. J., Bell, J. I., Stuart, D. I., and Jones, E. Y. (2003) *Nat Immunol* **4**, 657-663

42. Sliz, P., Michielin, O., Cerottini, J. C., Luescher, I., Romero, P., Karplus, M., and Wiley, D. C. (2001) *J Immunol* **167**, 3276-3284

43. Kjer-Nielsen, L., Clements, C. S., Purcell, A. W., Brooks, A. G., Whisstock, J. C., Burrows, S. R., McCluskey, J., and Rossjohn, J. (2003) *Immunity* **18**, 53-64

44. Borbulevych, O. Y., Insaidoo, F. K., Baxter, T. K., Powell, D. J., Jr., Johnson, L. A., Restifo, N. P., and Baker, B. M. (2007) *J Mol Biol* **372**, 1123-1136

45. Valmori, D., Dutoit, V., Lienard, D., Lejeune, F., Speiser, D., Rimoldi, D., Cerundolo, V., Dietrich, P. Y., Cerottini, J. C., and Romero, P. (2000) *J Immunol* **165**, 533-538
46. Turner, S. J., Doherty, P. C., McCluskey, J., and Rossjohn, J. (2006) *Nat Rev Immunol* **6**, 883-894
47. Yoshioka, T., Matsutani, T., Iwagami, S., Tsuruta, Y., Kaneshige, T., Toyosaki, T., and Suzuki, R. (1997) *J Immunol Methods* **201**, 145-155
48. Tynan, F. E., Burrows, S. R., Buckle, A. M., Clements, C. S., Borg, N. A., Miles, J. J., Beddoe, T., Whisstock, J. C., Wilce, M. C., Silins, S. L., Burrows, J. M., Kjer-Nielsen, L., Kostenko, L., Purcell, A. W., McCluskey, J., and Rossjohn, J. (2005) *Nat Immunol* **6**, 1114-1122
49. Armstrong, K. M., Insaidoo, F. K., and Baker, B. M. (2008) *J Mol Recognit* **21**, 275-287
50. Miles, J. J., Silins, S. L., and Burrows, S. R. (2006) *Curr Med Chem* **13**, 2725-2736

**Table 1.** Data collection and refinement statistics (molecular replacement).

| Data set statistics (highest resolution shell in parenthesis) | |
|---|---|
| Space Group | P4$_3$ |
| Unit Cell parameters (Å) | a=b 120.9, c=82.0 |
| Radiation Source | SRS 14.2 |
| Wavelength (Å) | 0.978 |
| Resolution (Å) | 3.0 (3.16 – 3.0) |
| Reflection observed | 80,204 (11,687) |
| Unique reflections | 23,764 (3,464) |
| Completeness (%) | 99.5 (100.0) |
| Multiplicity | 3.4 (3.4) |
| I/Sigma(I) | 8.0 (1.6) |
| Rmerge (%) | 15.1 (79.4) |
| Refinement statistics (highest resolution shell in parenthesis) | |
| Measured Resolution Range (Å) | 48.7 – 3.0 |
| No reflections used | 22,525 (1,652) |
| No reflections in Rfree set | 1,211 (88) |
| Rcryst (no cutoff) (%) | 22.5 |
| Rfree (%) | 30.4 |
| RMSD from ideal geometry (target values in parenthesis) | |
| Bond lengths (Å) | 0.02 (0.021) |
| Bond Angles (°) | 1.2 (1.936) |
| Mean B value (Å$^2$) | 40.5 |
| Wilson B-factor (Å2) | 47.6 |
| Overall coordinate error(Å) | 0.4 |

One crystal was used for data collection.
*Values in parentheses are for highest-resolution shell.

**Table 2.** MEL5/A2-ELA contacts.

| CDR loop | TCR residue | Peptide residue | MHC residue | Bond Type | Bond Distance (Å) |
|---|---|---|---|---|---|
| CDR1α | Arg28$^{N\varepsilon}$ | | Glu166$^{O\varepsilon2}$ | Electrostatic | 3.4 |
| | Arg28$^{NH2}$ | | Glu166$^{O\varepsilon2}$ | Electrostatic | 3.1 |
| | Arg28$^{O}$ | | Trp167$^{N\varepsilon1}$ | Electrostatic | 3.7 |
| | Arg28$^{NH2}$ | | Glu166$^{O\varepsilon1}$ | Electrostatic | 3.5 |
| | Gln31$^{N\varepsilon2}$ | Glu1$^{O\varepsilon2}$ | | Electrostatic | 3.4 |
| | Gln31$^{N\varepsilon2}$ | Leu2$^{O}$ | | Electrostatic | 3.4 |
| | Gln31$^{C\delta}$ | Gly4$^{N}$ | | vdW | 3.3 |
| | Gln31$^{O\varepsilon1}$ | Gly4$^{C\alpha}$ | | vdW | 3.0 |
| | Gln31$^{O\varepsilon1}$ | Gly4$^{N}$ | | Electrostatic | 2.5 |
| | Gln31$^{O\varepsilon1}$ | Ile5$^{N}$ | | Electrostatic | 3.5 |
| CDR2α | Tyr51$^{OH}$ | | His151$^{O}$ | Electrostatic | 3.9 |
| CDR3α | Asn92$^{N\delta2}$ | Gly4$^{O}$ | | Electrostatic | 3.2 |
| CDR2β | Gln55$^{O\varepsilon1}$ | | Arg75$^{NH1}$ | Electrostatic | 3.3 |
| | Glu59$^{O\varepsilon1}$ | | Arg65$^{NH1}$ | Electrostatic | 2.8 |
| | Glu59$^{O\varepsilon2}$ | | Arg65$^{NH1}$ | Electrostatic | 3.5 |
| | Glu59$^{C\delta}$ | | Arg65$^{NH1}$ | vdW | 3.4 |
| CDR3β | Gly97$^{C\alpha}$ | | Thr73$^{C\gamma2}$ | vdW | 2.9 |
| | Gly99$^{C\alpha}$ | | Gln155$^{O\varepsilon1}$ | vdW | 3.4 |
| | Thr100$^{N}$ | | Gln155$^{O\varepsilon1}$ | Electrostatic | 2.9 |
| | Thr96$^{O\gamma1}$ | Thr9$^{O\gamma1}$ | | Electrostatic | 3.8 |
| | Leu98$^{C\gamma2}$ | Ala3$^{O}$ | | vdW | 3.3 |
| | Leu98$^{O}$ | Gly4$^{O}$ | | vdW | 3.2 |
| | Leu98$^{O}$ | Ile5$^{C\alpha}$ | | vdW | 3.2 |
| | Leu98$^{O}$ | Gly6$^{N}$ | | Electrostatic | 3.9 |
| | Leu98$^{O}$ | Ile7$^{N}$ | | Electrostatic | 3.8 |
| | Leu98$^{N}$ | Ile7$^{O}$ | | Electrostatic | 3.2 |
| | Gly99$^{N}$ | Ile7$^{O}$ | | Electrostatic | 3.4 |
| | Gly99$^{O}$ | Ile5$^{C\alpha}$ | | vdW | 3.3 |
| | Gly99$^{O}$ | Ile5$^{C\gamma2}$ | | vdW | 3.3 |

Contacts were calculated using a 4Å cut-off.

vdW – non-polar van der Waals contacts

Electrostatic – polar contacts

**Table 3.** Thermodynamic analysis of the MEL5/A2-ELA interaction.

| Temp (ºC) | 25 |
|---|---|
| $K_D$ (µM) | 18 |
| $\Delta G_0$ (kcal/mol) | -6.5 |
| $\Delta H_0$ (kcal/mol) | 2 |
| $T\Delta S_0$ (kcal/mol) | 8.3 |
| $\Delta Cp_0$ (kcal/mol·k) | -0.14 |

## Figure Legends

### Figure 1

**A** – The co-crystal structure of MEL5 (α chain shown as yellow cartoon, β chain shown as salmon cartoon) bound to the HLA-A*0201 (shown as green and blue cartoon) molecule complexed with the ELAGIGILTV peptide (shown as blue sticks). **B** – Expanded view of the interface between the MEL5 variable domain bound to the A2-ELA surface (colors as in 1A). The overall conformation of the ELAGIGILTV peptide (N- to C-terminus, left to right), including the central peptide bulge, is displayed. **C** – View from above of the MEL5 CDR loops bound to the A2-ELA surface (colors as in 1A, MEL5 CDR loops shown as spheres). The MEL5 TCR binds towards the N-terminus of the peptide, making contacts with the peptide via its CDR1 and CDR3 loops and contacts with the MHC surface via its CDR1 and CDR2 loops.

### Figure 2

**A** – The interactions between the CDR loops of MEL5 α chain (shown as yellow sticks) and the ELAGIGILTV peptide (shown as blue sticks). Electrostatic interactions are depicted as black dotted lines and vdW interactions are shown as red dotted lines. **B** – The interactions between the CDR loops of MEL5 β chain (shown as salmon sticks) and the ELAGIGILTV peptide (shown as blue sticks). Electrostatic interactions are depicted as black dotted lines and vdW interactions are shown as red dotted lines.

### Figure 3

**A** – The position of the CDR1α and CDR2α loops, encoded by the *TRAV12-2* gene, of MEL5 (shown as yellow spheres) in the HLA-A*0201 (shown as green cartoon) ELAGIGILTV peptide (shown as blue sticks) complex. **B** – The position of the CDR1α and CDR2α loops, encoded by the *TRAV12-2* gene, of the A6 TCR (shown as orange spheres) in the HLA-A*0201 (shown as blue cartoon) LLFGYPVYV peptide (shown as red sticks) complex. **C** – The conserved interactions (shown as dotted lines) between the CDR1α and CDR2α loops, encoded by the *TRAV12-2* gene, of MEL5 (shown as yellow sticks) and the HLA-A*0201 (shown as green sticks) ELAGIGILTV peptide (shown as blue sticks) complex. **D** – The conserved interactions (shown as dotted lines) between the CDR1α and CDR2α loops, encoded by the *TRAV12-2* gene, of the A6 TCR (shown as orange sticks) and the HLA-A*0201 (shown as blue sticks) LLFGYPVYV peptide (shown as red sticks) complex.

### Figure 4

The binding affinity and thermodynamics of the MEL5/A2-ELA interaction (A – G). These data were produced by surface plasmon resonance experiments using a BIAcore T100™ machine, which were then analyzed using equilibrium analysis and thermodynamic analysis using the Gibbs equation. The raw data and the fits are shown in each panel. These data illustrate the unusual thermodynamic properties of the MEL5/A2-ELA interaction (G).
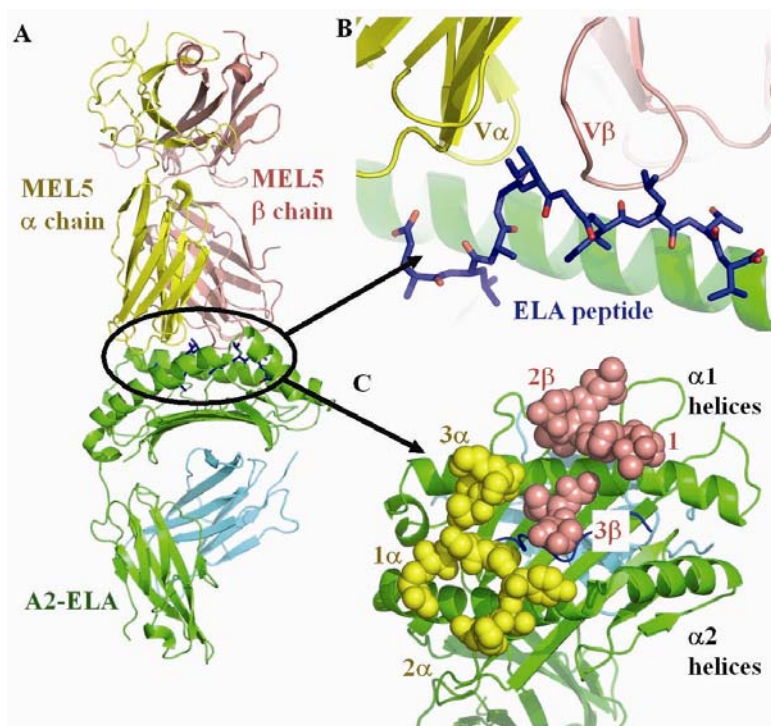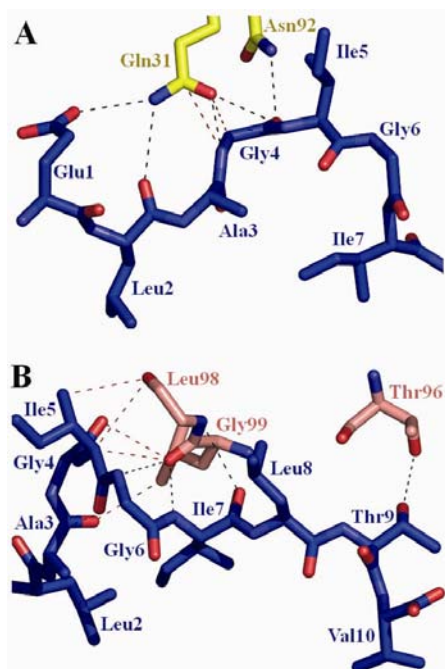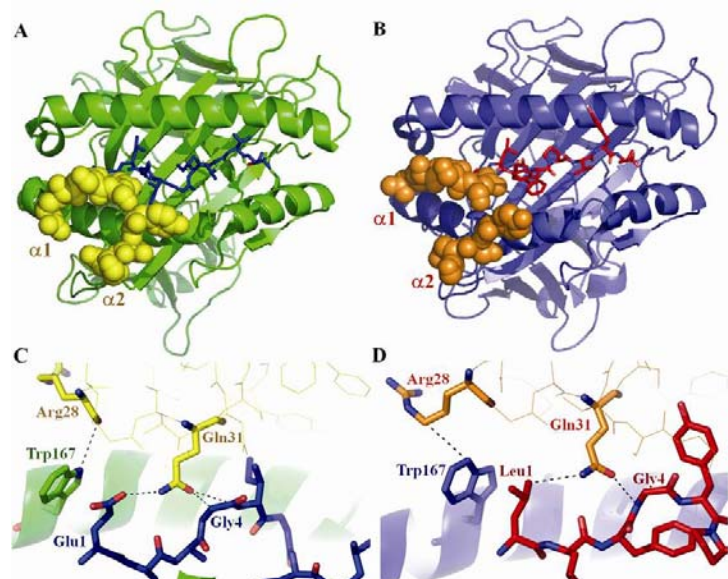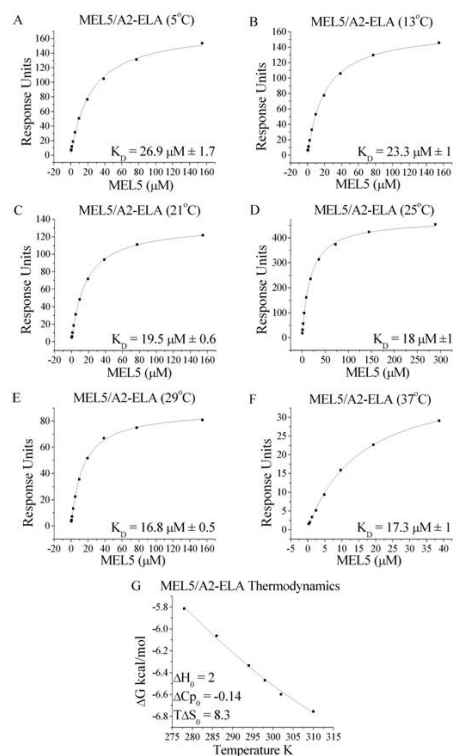
Figure 1



Figure 2

Figure 3



Figure 4